

04,10,15

## Impedance and dielectric spectra under alternating excitation of quasi-binary system of intercalated phases (Ag,Cu)–HfSe<sub>2</sub>

© V.G. Pleshchev

Institute of Natural Sciences, B.N. Yeltsin Ural Federal University, Ekaterinburg, Russia

E-mail: v.g.pleshchev@urfu.ru

Received March 17, 2025

Revised June 18, 2025

Accepted June 19, 2025

Relaxation processes during charge transfer and dipole polarization change under alternating excitation in hafnium diselenide when it is intercalated with atoms of two varieties Cu<sub>x</sub>Ag<sub>y</sub>HfSe<sub>2</sub> at  $(x + y) \leq 0.2$  have been studied by impedance spectroscopy. Based on the results of studies by impedance spectroscopy, relaxation processes in the system of mobile charge carriers were analyzed depending on the total content of intercalated atoms and the ratio of the number of atoms of different grades.

The dielectric characteristics of this system were analyzed for the first time. It is shown that at significant growth of dielectric permittivity in the region of low frequencies more informative for the analysis of dielectric relaxation is the use of the dielectric modulus formalism, on the basis of which the dielectric relaxation times are estimated. These times turned out to be smaller in comparison with the values determined from the frequency dependences of the imaginary part of the complex impedance.

**Keywords:** silver, copper, intercalation, hafnium diselenide, relaxation times, dielectric constant, electrical modulus.

DOI: 10.61011/PSS.2025.06.61685.50-25

### 1. Introduction

Layered transition metal dichalcogenides (LTMD) with general formula  $MX_2$  have been recently of high interest for research in field of functional materials science because they can be used for a wide range of applications [1–3]. Depending on the nature of transition metal and chalcogen,  $MX_2$  compounds exhibit various electrical properties from metallic to semiconductor ones. Owing to this, many of these materials may be used as electroactive components in electrical devices, as active contacts and electrode materials in electrochemical cells [4,5]. Electrical, magnetic and other properties of these materials are in direct relation to the concentration of interstitial atoms and the pattern of interaction with each other and with matrix compound atoms. Weak Van der Waals interaction between layers allows various methods for three-layer packing in a crystal along the axis perpendicular to the layers. Therefore, many LTMDs exist in several modifications and demonstrate various polytypes. In particular, hafnium diselenide as a chemical and structural equivalent of titanium diselenide has the 1T modification, where its lattice cell consists of one HfSe<sub>2</sub> layer, and metal atoms occupy octahedral sites [6,7]. Materials intercalated by copper and silver atoms are distinguished from intercalated 3-d transition elements. This is due to the fact that these ions in a wide range of binary and ternary compounds have high mobility owing to structural disorder [8]. Intercalated Cu<sub>x</sub>TiS<sub>2</sub> compounds were used as example to show that copper ions are weakly connected to the matrix layers due

to spherical distribution of electron density [9]. Therefore, charge transfer processes may be related not only to the contribution of electron carriers to conductivity, but also to ion motion. Electrochemical EMF method first used by the authors of [10] for examination of Ag<sub>x</sub>HfSe<sub>2</sub> samples also supported the conclusion concerning silver ion mobility in these compounds made earlier according to polarization phenomena observation data [11].

Employment of an impedance spectroscopy technique served as the advancement of kinetic property investigations of intercalated materials [10,12,13]. Such experiments can determine various complex quantities, including impedance, permittivity, electrical module, electric capacity. Various representations of AC material analysis data open new aspects for investigating the properties of such materials. Thus, according to such investigations for Ag<sub>x</sub>HfSe<sub>2</sub> ( $x = 0.1, 0.2$ ), the presence of mixed electronic–ionic conductivity was confirmed and electronic and ionic transfer numbers were evaluated for these compounds [13].

Examination of impedance properties on the Ag<sub>x</sub>HfSe<sub>2</sub> and Cu<sub>x</sub>HfSe<sub>2</sub> samples in a wide frequency range has shown that in both cases relaxation processes characterizing the charge transfer run more intensively when the copper or silver concentration in the samples increases [10,12]. However, relaxation times in silver-intercalated samples turn out to be several times as short as those in copper-intercalated ones, which confirms a higher silver ion mobility in these compounds. These differences also relate to the permittivity of copper-containing and silver-

containing intercalated compounds on the basis of hafnium dichalcogenides [14,15].

According to the existing literature, further investigations of chalcogenide transition metal compounds containing Group 1 elements are of real interest. For the purpose of advancement of the previous investigations using variable electric excitation, this work was focused not only on the charge transfer aspects, but also on previously unexplored dielectric properties of hafnium diselenide with joint (mixed) intercalation by copper and silver atoms in different ratios.

## 2. Experiment

Samples with mixed intercalation  $\text{Ag}_x\text{Cu}_y\text{HfSe}_2$  ( $x = 0.025, 0.05, 0.1$ ;  $y = 0.025, 0.05, 0.1$ ) were prepared from the preliminary synthesized and qualified series of  $\text{Ag}_x\text{HfSe}_2$  and  $\text{Cu}_y\text{HfSe}_2$  materials according to previously described techniques [12–14]. Mole fractions of each of the compounds in mixed phases were determined by accurately weighed feedstock using the known ratios of mass and molar amounts of the mixture components. The prepared mixtures were compacted and subjected to repeated annealing in quartz tubes at  $T = 850^\circ\text{C}$  until the desired composition homogeneity was achieved and confirmed by radiographic data on at least three different fragments from the prepared materials. For cooling after final annealing, the tubes with samples were quenched in ice water. The materials thus prepared were solid solutions in a quasi-binary system with static distribution of different grades of intercalated atoms between the  $\text{HfSe}_2$  layers. Impedance analyses were carried out at room temperature ( $T = 296 \pm 2$ ) K in the linear frequency range ( $f$ ) from 10 Hz to 5 MHz using the Solartron 1260A analyzer. The excitation signal amplitude in all cases was 0.05 V. The measurement data was analyzed within an equivalent circuit with paralleled resistor and capacitor whose capacity was mainly defined by the dielectric properties of the test samples.

The measurement samples had a form of tablets 10.5 mm in diameter and from 2.1 to 2.5 mm in thickness. The samples were placed between contacts in the form of plane-parallel plates. To reduce the edge effects, the diameter of contacts was twice as large as that of the samples. The space between the contacts may be represented in the form of two parallel capacitors, one of which is filled with dielectric and the other is empty. Further calculations of dielectric properties based on the complex impedance data used the electric capacities of the empty cell corresponding to the specified dimensions of the samples.

## 3. Research Results

Impedance spectra were measured for the  $\text{Ag}_x\text{Cu}_y\text{HfSe}_2$  samples with different ratios of different grades of atoms as shown in Figure 1. It can be seen that numerical

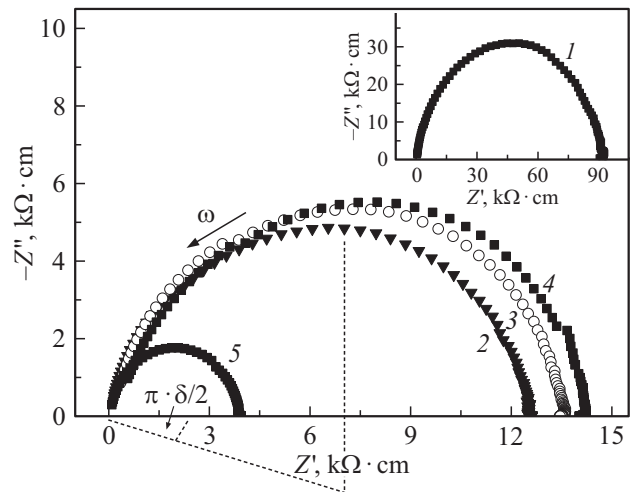


**Figure 1.** Complex impedance spectra  $\text{Ag}_{0.025}\text{Cu}_{0.025}\text{HfSe}_2$  (1),  $\text{Ag}_{0.025}\text{Cu}_{0.05}\text{HfSe}_2$  (2),  $\text{Ag}_{0.05}\text{Cu}_{0.05}\text{HfSe}_2$  (3),  $\text{Ag}_{0.05}\text{Cu}_{0.025}\text{HfSe}_2$  (4),  $\text{Ag}_{0.1}\text{Cu}_{0.1}\text{HfSe}_2$  (5).

value of the active electrical resistance ( $R_a = Z'$  at  $f \rightarrow 0$ ) depends on the total intercalated atoms as well as on the ratio of atoms. Being typical of the parallel equivalent circuit, the represented spectra have the form of arcs of circles. Within this circuit, the real and imaginary components of the complex impedance and cyclic frequency  $\omega = 2\pi f$  are interconnected as  $-Z'' = \omega R_a C_p Z'$  where  $R_a$  and  $C_p$  are the equivalent circuit elements [16]. When the impedance godograf is a full semicircle, then, at a frequency corresponding to the vertex of arc,  $Z' = |-Z''|$  and the time constant  $RC$  of the circuit (relaxation time) has some certain value equal to  $1/(R_a C_p)$ .

As shown in Figure 1, the  $\text{Ag}_x\text{Cu}_y\text{HfSe}_2$  spectra are shifted down along the imaginary axis and the centers of the arcs of circles lie below the real axis. This is the evidence of the fact that the provided results can not be interpreted within the Debye relaxation process model with frequency-independent resistances and capacities, and system-unique relaxation time. Possible participation in the charge transfer of electrons together with different types of ions [10,12,13] implies that there are processes with different relaxation properties. Since these contributions cannot be explicitly identified on the impedance spectra with the required certainty, this gives reason to consider continuous distribution of the equivalent RC-circuit parameters near some most probable (effective) value, instead of discrete contributions to the charge transfer. Width of the parameter distribution region and, therefore, of the relaxation time region may be evaluated by the angle  $\pi\delta/2$  between the  $Z'$  axis and the circle radius from the left end of the spectrum (at  $f \rightarrow \infty$ ) to the center of these circles as illustrated in Figure 1 for one of the spectra. In accordance with these representations,  $\delta$  quantitatively characterizes the degree of relaxation process deviation from the Debye model [17]. Such evaluation has

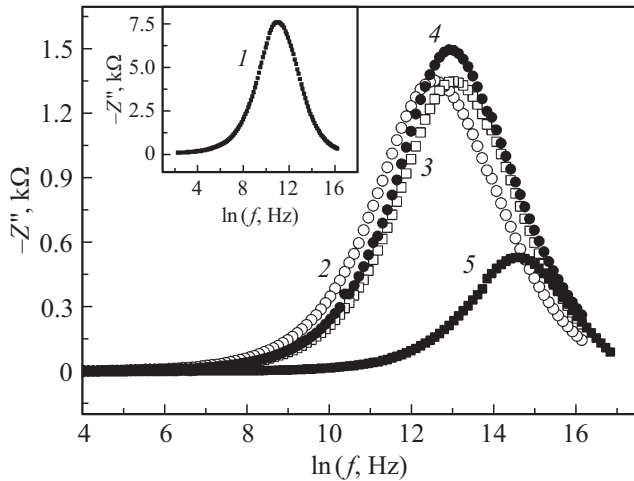


**Figure 2.** Frequency dependences of the complex impedance imaginary part  $\text{Ag}_{0.025}\text{Cu}_{0.025}\text{HfSe}_2$  (1),  $\text{Ag}_{0.025}\text{Cu}_{0.05}\text{HfSe}_2$  (2),  $\text{Ag}_{0.05}\text{Cu}_{0.05}\text{HfSe}_2$  (3),  $\text{Ag}_{0.05}\text{Cu}_{0.025}\text{HfSe}_2$  (4),  $\text{Ag}_{0.1}\text{Cu}_{0.1}\text{HfSe}_2$  (5).

shown that  $\delta$  decreased by a factor of 2 as the copper and silver concentration in the samples increased (Table).

Frequencies  $f_{\text{max}}^Z$ , at which the imaginary component of the impedance in Figure 1 has the maximum values, were more accurately determined by the frequency dependences of the imaginary component as shown in Figure 2.

According to the obtained data, above-mentioned ratio and actual real and imaginary components of impedance at  $f_{\text{max}}^Z$ , effective relaxation times  $\tau_Z$  were calculated for each composition as  $\tau_Z = |-Z''(\omega_m)|/\omega_m \cdot Z'(\omega_m)$ , where  $\omega_m = 2\pi f_{\text{max}}^Z$ . The results are shown in the table.

Analyzing the obtained parameters for different compounds, a conclusion may be made that  $\tau_Z$  in the given compounds with mixed intercalation vary not only when the total content of copper and silver varies, but also when the quantitative ratio between them varies. In addition, these relaxation times for the jointly intercalated  $\text{Ag}_x\text{Cu}_y\text{HfSe}_2$  compounds turn out to be shorter than those found before for copper-containing and silver-containing compounds individually with concentrations of intercalated atoms that are comparable with those for joint intercalation [10,12]. The highest  $\delta$  for the compound with the lowest silver and copper concentrations may be explained by the fact that in

Linear frequencies corresponding to the maximum imaginary parts of impedance ( $f_{\text{max}}^Z$ ) and electrical module ( $f_{\text{max}}^M$ ), relaxation times ( $\tau_Z$ ) and relaxation time distribution region index ( $\delta$ ) for the  $\text{Ag}_x\text{Cu}_y\text{HfSe}_2$  compounds

Compound	$f_{\text{max}}^Z$ , kHz	$\tau_Z$ , $\mu\text{s}$	$\delta$	$f_{\text{max}}^M$ , kHz	$\tau_M$ , $\mu\text{s}$
$\text{Ag}_{0.025}\text{Cu}_{0.025}\text{HfSe}_2$	55.8	1.94	0.24	315	0.51
$\text{Ag}_{0.025}\text{Cu}_{0.05}\text{HfSe}_2$	250.2	0.415	0.16	790	0.22
$\text{Ag}_{0.05}\text{Cu}_{0.05}\text{HfSe}_2$	446	0.26	0.17	995	0.16
$\text{Ag}_{0.05}\text{Cu}_{0.025}\text{HfSe}_2$	398	0.32	0.19	926	0.17
$\text{Ag}_{0.1}\text{Cu}_{0.1}\text{HfSe}_2$	1982	0.08	0.09	2810	0.06

this case these ions in electric field may move independently of each other, thus, providing different contributions to the width of the circuit parameter frequency distribution region. As the concentration of intercalated elements in interlayer spaces increases, motion of the intercalated elements in the external field shielding process may become more correlated due to the interaction between the intercalated elements, which leads to a decrease in the numerical value of  $\delta$ .

The features and characteristics of the dielectric response are usually determined by the frequency dependences of the real and imaginary parts of complex permittivity, which exhibit a typical maximum ( $\epsilon''$ ) or a step ( $\epsilon'$ ). Data obtained for the complex impedance taking into account a geometrical cell capacity for each of the samples were used to determine real and imaginary parts of permittivity [16]. The calculations found significant frequency dispersion of real ( $\epsilon'$ ) and imaginary ( $\epsilon''$ ) parts of the complex permittivity. As shown in Figure 3, curves  $\epsilon''$  don't exhibit a maximum typical for dielectric loss, but decrease monotonously as the frequency grows. Complex-plane permittivity spectra in the studied frequency range as shown in Figure 4 don't exhibit any maximum typical of the Cole-Cole diagrams either. Similar diagrams without such maximum in the dielectric spectrum were also observed before for other materials [18–20].

The form of curves shown in Figures 3 and 4 can not allow them to be used for quantitative determination of dielectric relaxation properties, which may be due, in particular, to prevalence of the energy loss by charge transfer (conductivity) over the relaxation loss. Representation of results in the form of electrical module whose value is the reciprocal for complex permittivity.

$$M^* = 1/\epsilon^* = M' + i \cdot M''.$$

Electrical module formalism makes it possible to identify the intrinsic dielectric behavior of the given mate-

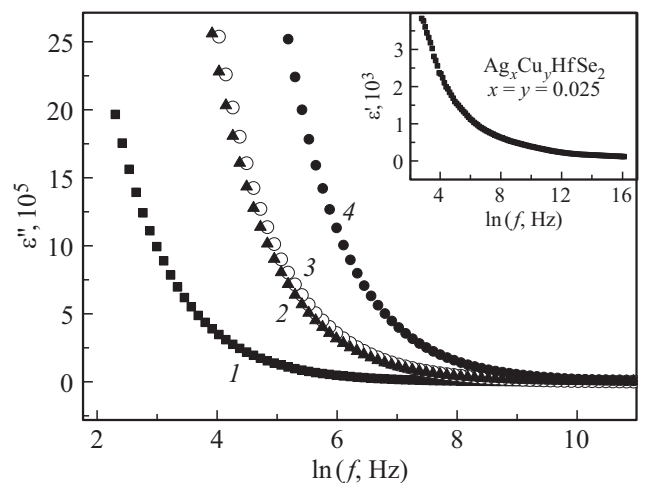


**Figure 3.** Frequency dependences of the real part of permittivity for  $\text{Ag}_{0.025}\text{Cu}_{0.025}\text{HfSe}_2$  (see the inset) and of the imaginary parts of permittivity.  $\text{Ag}_{0.025}\text{Cu}_{0.025}\text{HfSe}_2$  (1),  $\text{Ag}_{0.05}\text{Cu}_{0.025}\text{HfSe}_2$  (2),  $\text{Ag}_{0.025}\text{Cu}_{0.05}\text{HfSe}_2$  (3),  $\text{Ag}_{0.1}\text{Cu}_{0.1}\text{HfSe}_2$  (4).

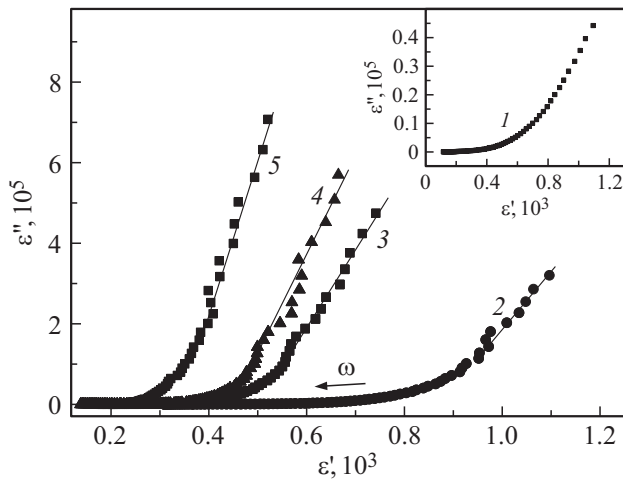


**Figure 4.** Permittivity spectra  $\text{Ag}_{0.025}\text{Cu}_{0.025}\text{HfSe}_2$  (1),  $\text{Ag}_{0.025}\text{Cu}_{0.05}\text{HfSe}_2$  (2),  $\text{Ag}_{0.05}\text{Cu}_{0.025}\text{HfSe}_2$  (3),  $\text{Ag}_{0.05}\text{Cu}_{0.05}\text{HfSe}_2$  (4),  $\text{Ag}_{0.1}\text{Cu}_{0.1}\text{HfSe}_2$  (5).

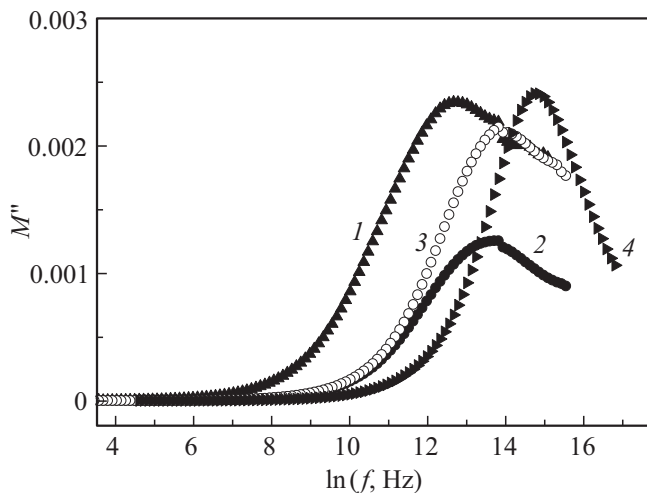


**Figure 5.** Frequency dependences of the imaginary parts of the complex electrical module of  $\text{Ag}_{0.025}\text{Cu}_{0.025}\text{HfSe}_2$  (1),  $\text{Ag}_{0.025}\text{Cu}_{0.05}\text{HfSe}_2$  (2),  $\text{Ag}_{0.05}\text{Cu}_{0.05}\text{HfSe}_2$  (3),  $\text{Ag}_{0.1}\text{Cu}_{0.1}\text{HfSe}_2$  (4).

rials through conversion of the monotonic permittivity variation into a relaxation peak, whose position on the frequency axis may be used to determine the dielectric relaxation time ( $\tau_\epsilon$ ) [21,22]. These conversions showed that  $M'' = \epsilon'' / (\epsilon''^2 + \epsilon'^2)$  really exhibits its maximum at a particular frequency as demonstrated in Figure 5. Typical dielectric relaxation times were found as  $\tau_\epsilon = (2\pi f_{\max}^M)^{-1}$  from  $f_{\max}^M$ , at which  $M'' = M''_{\max}$ . When the composition of  $\text{Ag}_x\text{Cu}_y\text{HfSe}_2$  varies, the frequency values as listed in the table vary in the same way as  $\tau_\epsilon$ , though remain 1.5 to 3 times as low as the latter. A difference between them decreases considerably as the total copper and silver concentration grows. These differences may be caused by the fact that the frequency dependences of the electrical module characterize bulk properties of crystallites to a

greater extent, but the influence of near-electrode processes and intercrystalline regions is reduced compared with the bulk properties. This is particularly typical of ion-conducting materials [10,13,23], and the compounds discussed in this work may be also classified as such.

## 4. Conclusion

The study jointly investigates kinetic and dielectric properties of materials simultaneously intercalated by silver and copper atoms. It is shown that the relaxation processes during charge transfer don't comply with the Debye model. Effective relaxation times characterizing the response of charge carriers to the excitation by a variable external electric field were determined taking into account specific location of the impedance spectra on the complex plane. In the given system, against the background of the general trend to decreasing the relaxation times with the growth of the total content of copper and silver, the ratio of the concentrations of intercalated atoms also affects their values. Taking into account that different grades of particles can participate in the charge transfer, the width of the equivalent circuit parameter distribution region was evaluated. Variations of the width are associated with the change of site population between the  $\text{HfSe}_2$  layers. At low concentrations, each grade of the intercalated atoms makes its independent contribution to the charge transfer with relaxation time typical for each of them, and as the content of copper and silver atoms increases, motion of the atoms in the external electric field becomes more coordinated due to the interaction between them.

The findings demonstrate considerable frequency dispersion of the permittivity of  $\text{Ag}_x\text{Cu}_y\text{HfSe}_2$  with monotonic frequency dependence of its real and imaginary parts. This prevents from using permittivity as a means for determining the dynamic response of dipole systems to external action of a variable electric field. This issue was overcome in this work by a calculation using the electrical module option that made it possible to convert the observed frequency growth of the permittivity into a relaxation peak. These conversions provided frequency dependences of the imaginary parts of the complex electrical module that pass through the maximum values at certain frequencies. Relaxation times determined using this data turned out to be lower for all studied compounds than those determined from the analysis of the frequency dependence of the complex impedance components.

## Funding

The work was supported by the Ministry of Science and Higher Education of the Russian Federation (State task No. FEUZ-2023-0017).

## Acknowledgments

We express our gratitude to N.V.Selezneva, Candidate of Physical and Mathematical Sciences, for her help in performing radiographic certification of the research objects.

## Conflict of interest

The author declares no conflict of interest.

## References

- [1] J. Shi, M. Hong, Z. Zhang, Q. Ji. *Coord. Chem. Rev.* **376**, 7, 1–19 (2018). DOI: 10.1016/j.ccr.2018.07.019
- [2] L. Song, H. Li, Y. Zhang, J. Shi. *J. Appl. Phys.* **131**, 11, 060902 (2022). <https://doi.org/10.1063/5.0083929>
- [3] A. Yu.Ledneva, G.E.Tchebanova, S.B.Artemkina, A.N.Lavrov. *Zhurnal strukturnoj khimii* **63**, 2, 109–162 (2022). (in Russian). DOI: 10.26902/JSC\_id87109
- [4] C.K. Sumesh, K.D. Patel, V.M. Pathak, R. Srivastava. *J. Electron Dev.* **8**, 324 (2010).
- [5] K.E. Aretouli, P. Tsipas, D. Tsoutsou, J. Marquez-Velasco, E. Xenogiannopoulou, S.A. Giamini, E. Vassalou, N. Kelaidis, A. Dimoulas. *Appl. Phys. Lett.* **106**, 143105 (2015). DOI: 10.1063/1.4917422
- [6] L.A. Chernozatonsky, A.A. Artyukh. *UFN* **188**, 1, 3 (2018). (in Russian). DOI: 10.3367/UFNr.2017.02.038065
- [7] P. Katzke, W. Toledano, W. Depmeier. *Phys. Rev. B* **69**, 134111 (2004). <https://doi.org/10.1103/PhysRevB.69.134111>
- [8] Yu.A. Gurevich. *Tverdyye elektrolity*. M: Nauka, 1986). 173 p. (in Russian).
- [9] A.H. Reshak. *J. Phys. Chem. A* **113**, 8, 1635–1645 (2009). DOI: 10.102/jp810242w
- [10] V.G. Pleshchev, N.V. Selezneva, N.V. Baranov. *Phys. Solid State*, **55**, 7, 1377 (2013). doi:10.1134/S1063783413070238
- [11] V.G. Pleshchev, N.V. Selezneva, N.V. Baranov. *Phys. Solid State* **55**, 1, 21 (2013). (DOI) 10.1134/S1063783413010253
- [12] V.G. Pleshchev, N.V. Selezneva, N.V. Melnikova, N.V. Baranov. *Phys. Solid State* **54**, 7, 1348 (2012). doi:10.1134/S1063783412070293
- [13] V.G. Pleshchev. *Phys. Solid State* **64**, 10, 1420 (2022). DOI: 10.21883/PSS.2022.10.54230.317
- [14] V.G. Pleshchev. *Phys. Solid State* **65**, 2, 224 (2023). doi: 10.21883/PSS.2023.02.55404.520
- [15] V.G. Pleshchev. *Phys. Solid State* **67**, 1, 130 (2025). doi: 10.61011/PSS.2025.01.60591.278
- [16] N.A. Poklonsky, N.I. Gorbachuk. *Osnovy impedansnoy spektroskopii kompozitov*. Izd-vo BGU, Minsk (2005). 50 p. (in Russian).
- [17] E. Barsoukov, J.R. Macdonald. *Impedance spectroscopy: theory, experiment and applications*. John Wiley & Sons Inc., N.J. (2005). 595 p.
- [18] M.Yu. Seyidov, R.A. Suleymanov, Y. Bakis, F. Salehli. *J. Appl. Phys.* **108**, 7, 074114(5) (2010). DOI: 10.1063/1.3486219
- [19] N.D. Gavrilova, A.M. Lotonov, A.A. Davydova. *Vestnik Moskovskogo universiteta. Seriya 3. Fizika. Astronomiya*, **1**, 45 (2013). (in Russian).
- [20] M.A. Kudryashov, A.I. Mashin, A.A. Logunov, G. Chidichimo, G. De Filpo. *ZhTF* **84**, 7, 67 (2014). (in Russian).
- [21] M.M. Costa, G.F.M. Pires, Jr., A.J. Terezo, M.P.F. Graca, S.B. Sombra. *J. Appl. Phys.* **110**, 034107 (2011). DOI: 10.1063/1.3615935
- [22] P.K. Karahaliou, N. Xanthopoulos, S. Georga. *Physica Scripta* **86**, 6, 065703 (2012). DOI: 10.1088/0031-8949/86/06/065703
- [23] S.R. Elliott. *J. Non-Cryst. Solids*. **170**, 1, 97 (1994). doi.org/10.1016/0022-3093(94)90108-2

*Translated by E.Ilnskaya*